Special Issue on "Theoretical and Computational Chemistry"

J. Indian Chem. Soc.,
Vol. 96, July 2019, pp. 863-868

Ultrafast intersystem crossing in naphthalene diimides: Involvement of higher triplet states

Sai Vamsi Krishna Isukapalli and Vennapusa Sivaranjana Reddy*

School of Chemistry, Indian Institute of Science Education and Research Thiruvananthapuram, Maruthamala PO, Vithura, Thiruvananthapuram-695 551, Kerala, India

E-mail: siva@iisertvm.ac.in

Manuscript received online 30 April 2019, revised and accepted 16 May 2019

Conventionally, the triplet state generation via S_1° $T_1$is thought to be the slowest molecular photophysical process in organic conjugated molecules. However, recent advanced experimental spectroscopic investigations by Yushchenko *et al*. [*J. Phys. Chem. Lett.*, 2012, **6**, 2096-2100] revealed an ultrafast triplet formation of bromo core substituted naphthalene diimide (rNDI). Here, we estimated various stationary points of the low-lying singlet-triplet manifold of prototype NDIs using model vibronic Hamiltonian to gain insights into the mechanistic details of intersystem crossing (ISC) pathways of rNDI. Several ISC pathways involving S_1 and S_2 are identified where the higher triplet states, T_n (n > 2) are found to be energetically more accessible than T_2 and T_1. Our findings of NDIs are correlated to interpret the experimental ISC findings of rNDI.

Keywords: Intersystem crossing, ultrafast triplet formation, energy gap law, linear vibronic coupling, stationary points.

Introduction

Internal conversion (IC) and intersystem crossing (ISC) are two competing nonradiative photophysical processes of a photoexcited molecule during its relaxation to the ground electronic state (S_0). If the molecule is excited to Franck-Condon (FC) point on S_2 state, then the molecule relaxes either to S_1 state via IC or directly to an isoenergetic receiver triplet state via ISC. The other triplet-state formation pathway is the ISC from vibronically relaxed S_1 state. The latter process is the conventional ISC pathway referred in the literature[1].

Recent experimental time-resolved nanosecond and femtosecond spectroscopic measurements revealed two different triplet generation timescales in amino and bromo core substituted red naphthalene diimide[2] (rNDI) (see Fig. 1). Fluorescence and triplet quantum yields were analyzed by exciting the molecule with S_2ü S_0 and S_1ü S_0 transition energies. The observed triplet formation timescale of <200 fs was attributed to the direct ISC from S_2 to triplet manifold. ISC involving S_1 state is found to be slower, occurring on nanosecond time regime.

A detailed theoretical study to elucidate the reported experimental ISC pathways of rNDI is a daunting task. This is primarily due to the challenge posed by the energetically close-lying excited electronic states, which tend to exhibit strong non-adiabatic effects. Moreover, the estimation of

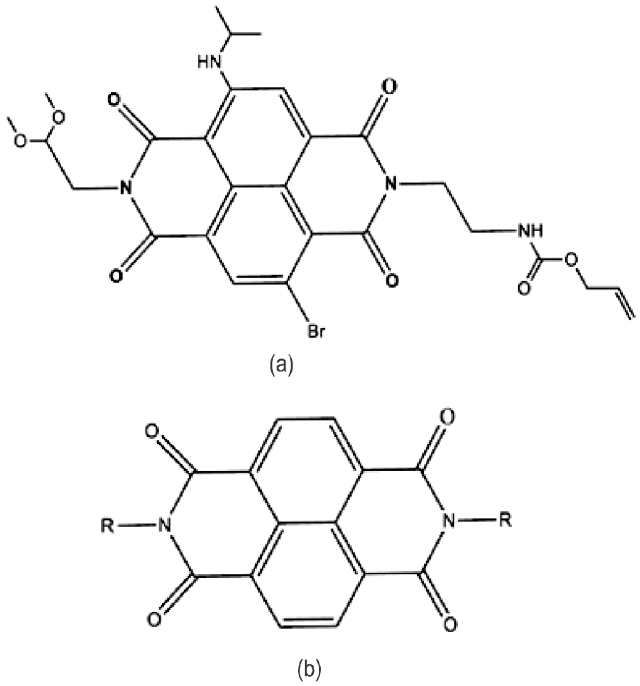

Fig. 1. Schematic diagram of (a) bromo and amino core substituted red naphthalenediimide, (rNDI) and (b) substituted NDI (R-NDI where R = H, Me).

various stationary points of excited-state potential energy surfaces requires expensive quantum chemical calculations and can be very time consuming. Hence, we choose prototype NDI derivatives (see Fig. 1) to provide insight into ISC pathways of reported rNDI.

Two steps are involved in this study: First, vertical excitation energies are computed at FC geometry i.e. S_0 equilibrium geometry, of each molecule to evaluate the singlet-triplet energy gaps. Such energy data is analyzed using energy gap law[3,4] to identify the energetically accessible receiver triplet states. Secondly, the location of global minima of low-lying singlet-triplet states with respect to FC point is the other factor which plays a key role in regulating ISC. In principle, excited-state optimization calculation could provide the minimum energy of the relevant state. However, such type of calculations are unfeasible owing to the complexity arising from the large number of vibrational degrees of freedom and near-degenerate electronic manifold, and are sometimes successful but not reliable. Hence, we employ a different strategy where simple model vibronic Hamiltonians within the well-established linear vibronic coupling[5–7] approach are constructed to estimate the global minima of the involved electronic states. The energy gap at FC geometry and at their respective minima of singlet-triplet manifold are taken into consideration for predicting the plausible ISC pathways in NDIs. Obtained outcomes are then correlated to interpret the experimental findings of rNDI.

Results and discussion

Geometry optimization: Ground-state equilibrium geometry optimization and vibrational frequency calculations of NDIs are performed using density functional theory (DFT). A hybrid density functional method, B3LYP[8] (Becke, three parameter, Lee-Yang-Parr), in combination with 6-311G* basis set is employed. Time-dependent DFT (TD-DFT) computations are carried out to evaluate the vertical excitation energies of singlet and triplet states of these molecules. All computations are carried out using Gaussian 09 software package[9].

Fig. 2 depicts the vertical excitation energies of NDIs. From this Fig. 2, it is evident that T_1 state is energetically well-separated from S_1, than the other triplet states, for all

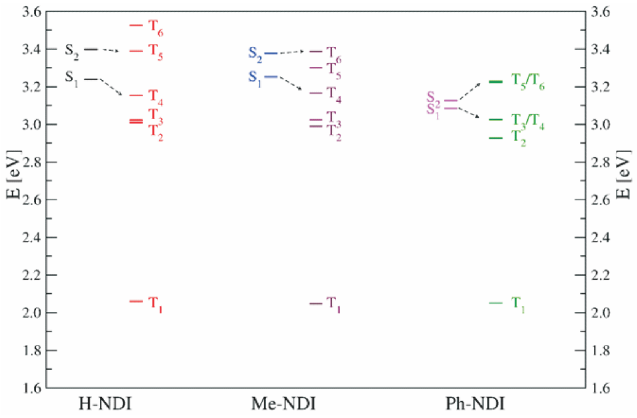

Fig. 2. Vertical excitation energies of low-lying electronic states of R-NDI computed at TD-B3LYP/6-311G* level of theory. Energetically favorable ISC pathways are shown with arrow symbol.

NDIs. Hence, S_1° T_1 ISC pathway is less favourable, compared to other higher triplet receiver states, based on the "energy gap law" – which states that the rate of nonradiative transition should increase with decrease of energy gap of involved electronic states. We found that S_1° T_4 in H- and Ph-NDI and S_1° T_5 in Me-NDI are likely to be the energetically most favourable ISC pathways. If ISC originates from S_2, then S_2° T_6 in H-NDI, S_2° T_5 in Me-NDI and Ph-NDI would become the favourable pathways.

Note that the ISC pathway identified at FC point of S_2 may compete with S_2° S_1 IC. The latter process become dominant as the S_2-S_1 energy gap decreases with the increase of molecular size (*cf.* Fig. 2). The energy gap trends suggest that S_2° T_5/T_6 ISC is favoured over S_2° S_1 IC for H- and Me-NDIs. For Ph-NDI, S_2° S_1 IC followed by ISC from S_1 becomes the favourable triplet generation pathway.

Here, we highlight that the receiver triplet state in these favoured pathways may vary if the molecule undergoes very fast intramolecular relaxation to the respective minimum of involved singlet states due to severe geometrical distortions upon photoexcitation. The energy associated with these geometrical distortions is called the stabilization/reorganization energy of the electronic state (E_s)[12]. Details of geometrical distortions and E_s could be obtained by performing optimization calculation for an excited state. However, such a calculation is computationally expensive. Thus, as stated above,

we adopt an alternate procedure where the linear vibronic coupling mechanism is employed to evaluate various stationary points of excited-states.

A 2×2 (for S_1-S_2 states) and 6×6 (for T_1-T_6 states) model Hamiltonians are constructed within the linear vibronic coupling using diabatic representation and symmetry selection rules[10]. For instance, the Hamiltonian for S_1-S_2 coupled states is given as:

$$H = (T_N + V_0)\, I_2 + \begin{pmatrix} E_1 + \kappa_1 Q_g & \lambda Q_u \\ \lambda Q_u & E_2 + \kappa_2 Q_g \end{pmatrix}$$

where T_N and V_0 represent the ground-state kinetic energy and potential energy terms. I_2 represents 2×2 identy matrix. The potential energy term is approximated to be harmonic potential with $V = S_i w_i Q_i^2$ where w is frequency and Q is the corresponding dimensionless normal coordinates[11] of vibration i. The totally and non-totally symmetric vibrational modes are represented by g and u, respectively. E_1 and E_2 are the FC vertical excitation energies of S_1 and S_2, respectively. The interstate (k) and intrastate (l) coupling parameters are estimated using below expressions:

$$\kappa^{(n)} = \left(\frac{\partial V_n(Q)}{\partial Q} \right)_{Q_0} ; \; n = 1,2$$

$$\lambda^{(1,2)} = \left\{ \frac{1}{8} \frac{\partial^2}{\partial Q^2} \{V_1(Q) - V_2(Q)\}^2 \right\}^{1/2}_{Q_0}$$

A computational approach for evaluating k and l may be found elsewhere[12] and is not discussed here for brevity. In the present study, we have followed this approach to estimate the parameters at TD-B3LYP/6-311G* level of theory. The coupling constant values of NDIs are collected in Tables 1-3. The stabilization energy E_s is calculated using the expression: $E_s = k^2/2w$.

A quantum dynamical study of coupled S_1-S_2 and T_1-T_6 states is out of the scope of the present study and is planned for future investigations.

Stationary points: To understand on how the electronic energies vary with the geometrical distortions, we have plotted adiabatic potential energies, obtained by diagonalization of the diabatic Hamiltonian along the dimensionless normal coordinates of C=O stretching vibration of H-NDI in Fig. 3.

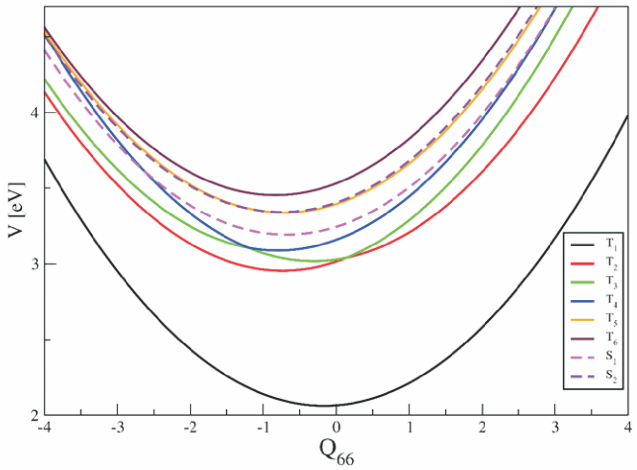

Fig. 3. Potential energy cuts of low-lying electronic states along C=O stretching mode (Q_{66}) of H-NDI.

Table 1. Intrastate coupling parameters (k) for excited singlet and triplet states for H-NDI. The stabilization energy (E_s) corresponding to each vibrational mode is shown in the parentheses. All values are in eV

Mode (freq)	S_1	S_2	T_1	T_2	T_3	T_4	T_5	T_6
ν_{10}(0.0386)	-0.0183(0.1126)	-0.0168(0.0942)	-0.0271(0.0246)	-0.0178(0.1064)	0.0073(0.0181)	-0.0080(0.0215)	-0.0145(0.0704)	-0.0270(0.2449)
ν_{14}(0.0524)	0.0627(0.7170)	0.0388(0.2743)	0.0156(0.0445)	0.0578(0.6077)	-0.0086(0.0136)	0.0572(0.5958)	0.0365(0.2421)	0.0327(0.1946)
ν_{20}(0.0687)	0.0020(0.0004)	-0.0123(0.0160)	-0.0352(0.1312)	0.0028(0.0008)	-0.0193(0.0395)	0.0069(0.0050)	-0.0282(0.0840)	-0.0039(0.0016)
ν_{26}(0.0871)	-0.0251(0.0416)	-0.0248(0.0405)	-0.0463(0.1415)	-0.0222(0.0326)	0.0108(0.0077)	-0.0158(0.0164	-0.0323(0.0688)	-0.0306(0.0617)
ν_{41}(0.1293)	-0.0418(0.0522)	-0.0460(0.0633)	-0.0566(0.0957)	-0.0440(0.0578)	-0.0909(0.2469)	-0.0510(0.0778)	-0.0508(0.0772)	-0.0694(0.1441)
ν_{44}(0.1418)	0.0533(0.0705)	0.0574(0.0820)	0.0333(0.0276)	0.0495(0.0608)	-0.0664(0.1095)	0.0528(0.0694)	0.0348(0.0302)	0.0355(0.0313)
ν_{50}(0.1659)	0.0686(0.0854)	0.0760(0.1048)	-0.0143(0.0037)	0.0639(0.0742)	0.0460(0.0384)	0.0692(0.0870)	0.0046(0.0004)	0.0150(0.0041)
ν_{53}(0.1743)	0.0097(0.0016)	0.0190(0.0059)	-0.1128(0.2093)	0.0108(0.0019)	-0.0057(0.0005)	0.0195(0.0062)	0.0359(0.0213)	-0.0672(0.0743)
ν_{54}(0.1775)	-0.1274(0.2575)	-0.1355(0.2913)	-0.1764(0.4940)	-0.1170(0.2171)	-0.1237(0.2428)	-0.1223(0.2373)	-0.0625(0.0620)	-0.0827(0.1086)
ν_{61}(0.2030)	0.1346(0.2197)	0.1510(0.2767)	0.2192(0.5830)	0.1299(0.2049)	0.0187(0.0042)	0.1239(0.1861)	0.2130(0.5506)	0.0700(0.0594)
ν_{66}(0.2211)	0.1507(0.2323)	0.1662(0.2824)	0.0364(0.0136)	0.1625(0.2702)	0.0688(0.0484)	0.1767(0.3194)	0.1573(0.2530)	0.1849(0.3497)
ν_{70}(0.3987)	-0.0015(0.0000)	-0.0070(0.0002)	-0.0101(0.0003)	-0.0010(0.0000)	-0.0097(0.0003)	-0.0062(0.0001)	-0.0049(0.0001)	-0.0072(0.0002)
ν_{72}(0.4448)	-0.0024(0.0000)	-0.0017(0.0000)	-0.0006(0.0000)	-0.0017(0.0000)	-0.0025(0.0000)	-0.0009(0.0000)	0.0006(0.0000)	0.0061(0.0001)

Table 2. Intrastate coupling parameters (k) for excited singlet and triplet states for Me-NDI. The stabilization energy (E_s) corresponding to each vibrational mode is shown in the parentheses. All values are in eV

Mode (freq)	S_1	S_2	T_1	T_2	T_3	T_4	T_5	T_6
ν_{12}(0.0365)	-0.0295(0.3259)	-0.0263(0.2598)	-0.0268(0.2701)	0.0006(0.0002)	-0.0282(0.2981)	-0.0210(0.1654)	-0.0227(0.1930)	-0.0112(0.0470)
ν_{14}(0.0388)	-0.0046(0.0070)	0.0025(0.0020)	0.0016(0.0008)	0.0001(0.0000)	-0.0045(0.0067)	-0.0048(0.0077)	0.0000(0.0000)	-0.0006(0.0001)
ν_{17}(0.0468)	0.0173(0.0686)	0.0008(0.0001)	0.0000(0.0000)	0.0005(0.0001)	0.0160(0.0586)	0.0176(0.0708)	0.0119(0.0324)	0.0105(0.0254)
ν_{19}(0.0509)	-0.0116(0.0259)	0.0012(0.0003)	0.0005(0.0000)	-0.0022(0.0009)	-0.0109(0.0231)	-0.0117(0.0263)	-0.0114(0.0249)	-0.0098(0.0185)
ν_{20}(0.0520)	0.0427(0.3372)	0.0002(0.0006)	0.0011(0.0002)	0.0059(0.0064)	0.0390(0.2812)	0.0424(0.3327)	0.0433(0.3466)	0.0381(0.2679)
ν_{26}(0.0688)	-0.0064(0.0044)	0.0330(0.1148)	0.0356(0.1336)	0.0215(0.0489)	-0.0068(0.0049)	-0.0110(0.0127)	0.0260(0.0715)	0.0261(0.0721)
ν_{29}(0.0767)	-0.0012(0.0001)	-0.0001(0.0000)	0.0005(0.0000)	0.0006(0.0000)	-0.0016(0.0002)	-0.0016(0.0002)	-0.0001(0.0000)	-0.0007(0.0000)
ν_{30}(0.0778)	0.0508(0.2135)	0.0298(0.0732)	0.0413(0.1407)	-0.0197(0.0319)	0.0458(0.1731)	0.0394(0.1283)	0.0071(0.0042)	-0.0007(0.0000)
ν_{39}(0.1064)	0.0001(0.0000)	-0.0002(0.0000)	0.0002(0.0000)	0.0006(0.0000)	0.0002(0.0000)	-0.0005(0.0000)	0.0030(0.0004)	0.0022(0.0002)
ν_{42}(0.1164)	0.0151(0.0085)	-0.0380(0.0532)	-0.0484(0.0866)	-0.0456(0.0767)	0.0117(0.0051)	0.0116(0.0050)	0.0292(0.0316)	0.0135(0.0068)
ν_{47}(0.1316)	0.0060(0.0010)	-0.0027(0.0002)	-0.0009(0.0000)	-0.0021(0.0001)	0.0057(0.0009)	0.0061(0.0011)	-0.0066(0.0013)	-0.0057(0.0009)
ν_{49}(0.1351)	0.0829(0.1883)	0.0329(0.0296)	0.0503(0.0693)	0.0490(0.0656)	0.0814(0.1814)	0.0893(0.2183)	0.0609(0.1017)	0.0535(0.0785)
ν_{52}(0.1457)	-0.0003(0.0000)	-0.0129(0.0039)	-0.0229(0.0124)	0.0780(0.1434)	0.0019(0.0001)	0.0039(0.0004)	-0.0110(0.0029)	0.0071(0.0012)
ν_{53}(0.1463)	0.0056(0.0007)	-0.0051(0.0006)	-0.0064(0.0009)	0.0218(0.0111)	0.0059(0.0008)	0.0058(0.0008)	-0.0036(0.0003)	0.0008(0.0000)
ν_{55}(0.1535)	0.0038(0.0003)	-0.0018(0.0001)	-0.0005(0.0000)	0.0020(0.0001)	0.0030(0.0002)	0.0025(0.0001)	0.0015(0.0001)	0.0015(0.0001)
ν_{58}(0.1619)	-0.0007(0.0000)	-0.0042(0.0003)	-0.0054(0.0006)	0.0019(0.0001)	-0.0007(0.0000)	0.0005(0.0000)	-0.0053(0.0005)	-0.0046(0.0004)
ν_{60}(0.1682)	0.0409(0.0295)	-0.0111(0.0022)	-0.0039(0.0003)	0.0390(0.0268)	0.0363(0.0233)	0.0391(0.0270)	0.0715(0.0905)	0.0701(0.0869)
ν_{63}(0.1741)	0.0245(0.0099)	-0.0451(0.0336)	-0.0553(0.0504)	0.0276(0.0125)	0.0228(0.0086)	0.0301(0.0150)	0.0706(0.0822)	0.0510(0.0429)
ν_{64}(0.1781)	0.1171(0.2160)	0.1662(0.4354)	0.2109(0.7008)	0.1179(0.2190)	0.1067(0.1794)	0.1104(0.1921)	0.1168(0.2152)	0.1199(0.2266)
ν_{66}(0.1816)	-0.0399(0.0242)	-0.0036(0.0002)	-0.0035(0.0002)	-0.0415(0.0262)	-0.0373(0.0211)	-0.0426(0.0275)	-0.0847(0.1088)	-0.0759(0.0874)
ν_{68}(0.1865)	0.0015(0.0000)	-0.0013(0.0000)	0.0002(0.0000)	0.0001(0.0000)	0.0007(0.0000)	0.0006(0.0000)	0.0001(0.0000)	-0.0003(0.0000)
ν_{72}(0.1885)	-0.0145(0.0029)	0.0049(0.0003)	0.0045(0.0003)	-0.0013(0.0000)	-0.0136(0.0026)	-0.0143(0.0029)	0.0003(0.0000)	0.0009(0.0000)
ν_{75}(0.2030)	0.1279(0.1986)	0.1674(0.3398)	0.2101(0.5357)	0.0268(0.0087)	0.1236(0.1855)	0.1189(0.1715)	0.1445(0.2532)	0.1292(0.2027)
ν_{76}(0.2052)	0.0036(0.0002)	0.0006(0.0000)	0.0042(0.0002)	0.0036(0.0002)	0.0035(0.0001)	0.0046(0.0002)	0.0024(0.0001)	0.0009(0.0000)
ν_{78}(0.2150)	0.0094(0.0010)	0.0098(0.0010)	-0.0001(0.0000)	-0.0010(0.0000)	0.0111(0.0013)	0.0119(0.0015)	-0.0052(0.0003)	-0.0017(0.0000)
ν_{80}(0.2195)	-0.1614(0.2704)	-0.0425(0.0187)	-0.0351(0.0127)	-0.0778(0.0628)	-0.1729(0.3101)	-0.1877(0.3655)	-0.1485(0.2288)	-0.1307(0.1772)
ν_{82}(0.3811)	-0.0023(0.0000)	-0.0011(0.0000)	-0.0007(0.0000)	-0.0017(0.0000)	-0.0029(0.0000)	-0.0034(0.0000)	-0.0066(0.0002)	-0.0064(0.0001)
ν_{86}(0.3964)	0.0039(0.0000)	0.0000(0.0000)	0.0000(0.0000)	-0.0005(0.0000)	0.0034(0.0000)	0.0039(0.0000)	-0.0043(0.0001)	-0.0039(0.0000)
ν_{88}(0.3974)	0.0001(0.0000)	0.0005(0.0000)	0.0004(0.0000)	0.0005(0.0000)	0.0001(0.0000)	0.0002(0.0000)	0.0001(0.0000)	0.0001(0.0000)
ν_{90}(0.3988)	0.0008(0.0000)	0.0085(0.0002)	0.0103(0.0003)	0.0090(0.0003)	0.0003(0.0000)	0.0052(0.0001)	0.0037(0.0000)	0.0049(0.0001)

The energy lowering of electronic states is evident from Fig. 3. For instance, the vertical excitation energy at FC geometry (Q = 0) of S_1 is ~3.24 eV and the minimum on S_1 potential curve is located at ~3.19 eV (corresponding Q_{66} = –0.7). The energy difference between these two stationary points is the E_s due to Q_{66}. For a better illustration, E_s is represented along with other stationary points in Fig. 4. Symmetry selection rules allows only the totally-symmetric vibrations would contribute to E_s. Total E_s (E_{st}) is taken as an additive quantity, i.e. the contribution from each of the totally symmetric vibrational mode. Estimated E_{st} values of NDIs are given in Table 4.

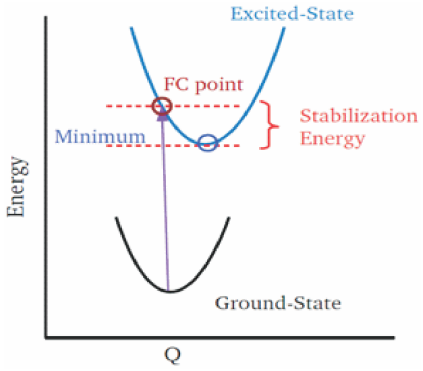

Fig. 4. Stationary points of an excited state of a molecule.

Table 3. Intrastate coupling parameters (k) for excited singlet and triplet states for Ph-NDI. The stabilization energy (E_s) corresponding to each vibrational mode is shown in the parentheses. All values are in eV

Mode (freq)	S_1	S_2	T_1	T_2	T_3	T_4	T_5	T_6
ν_{12}(0.0219)	-0.0416(1.8010)	-0.0463(2.2380)	-0.0130(0.1749)	-0.0316(1.0412)	-0.0015(0.0023)	-0.0371(1.4311)	-0.0256(0.6807)	-0.0250(0.6521)
ν_{21}(0.0430)	0.0485(0.6351)	0.0519(0.7291)	-0.0130(0.1749)	-0.0316(1.0412)	-0.0015(0.0023)	-0.0371(1.4311)	-0.0256(0.6807)	-0.0250(0.6521)
ν_{33}(0.0645)	-0.0745(0.6679)	-0.0637(0.4871)	-0.0309(0.1151)	-0.0728(0.6378)	-0.0711(0.6071)	0.0103(0.0127)	-0.0775(0.7214)	-0.0811(0.7911)
ν_{35}(0.0679)	0.0031(0.0011)	-0.0137(0.0204)	-0.0293(0.0931)	0.0179(0.0348)	0.0111(0.0135)	-0.0223(0.0541)	-0.0377(0.1542)	-0.0380(0.1564)
ν_{42}(0.0824)	0.0090(0.0059)	-0.0011(0.0001)	0.0332(0.0811)	0.0180(0.0239)	0.0098(0.0070)	-0.0102(0.0077)	-0.0753(0.4174)	-0.0635(0.2967)
ν_{55}(0.1037)	0.0588(0.1609)	0.0723(0.2428)	-0.0357(0.0594)	0.0335(0.0523)	0.0501(0.1166)	-0.0154(0.0110)	0.0278(0.0360)	0.0279(0.0362)
ν_{71}(0.1267)	0.0205(0.0131)	0.0240(0.0180)	0.0080(0.0020)	0.0139(0.0060)	0.0185(0.0107)	0.0122(0.0046)	0.0259(0.0210)	0.0257(0.0206)
ν_{73}(0.1290)	0.0529(0.0841)	0.0567(0.0967)	0.0448(0.0604)	0.0449(0.0606)	0.0530(0.0845)	0.0651(0.1274)	0.0580(0.1012)	0.0579(0.1008)
ν_{75}(0.1308)	-0.0365(0.0390)	-0.0301(0.0264)	-0.0326(0.0311)	-0.0401(0.0470)	-0.0406(0.0483)	-0.0466(0.0634)	-0.0099(0.0029)	-0.0098(0.0028)
ν_{78}(0.1404)	0.0381(0.0368)	0.0289(0.0212)	0.0334(0.0282)	0.0478(0.0581)	-0.0370(0.0348)	0.0407(0.0420)	0.0206(0.0107)	0.0208(0.0109)
ν_{84}(0.1488)	-0.0179(0.0073)	-0.0244(0.0135)	-0.0029(0.0002)	-0.0035(0.0003)	-0.0120(0.0033)	0.0137(0.0042)	0.0575(0.0747)	0.0328(0.0242)
ν_{88}(0.1523)	0.0323(0.0225)	0.0217(0.0101)	-0.0161(0.0056)	0.0396(0.0339)	0.0372(0.0299)	0.0676(0.0986)	-0.0326(0.0229)	-0.0343(0.0254)
ν_{94}(0.1677)	-0.0355(0.0224)	-0.0523(0.0487)	0.0004(0.0000)	-0.0248(0.0110)	-0.0306(0.0166)	-0.0361(0.0232)	-0.0868(0.1340)	-0.0885(0.1393)
ν_{99}(0.1739)	0.0233(0.0090)	0.0364(0.0218)	-0.0531(0.0467)	0.0167(0.0046)	0.0224(0.0083)	0.0303(0.0152)	0.0538(0.0479)	0.0532(0.0469)
ν_{100}(0.1780)	-0.1256(0.2490)	-0.1361(0.2924)	-0.2096(0.6932)	-0.1098(0.1902)	-0.1213(0.2322)	-0.1178(0.2190)	-0.1342(0.2843)	-0.1347(0.2865)
ν_{106}(0.1903)	-0.0021(0.0001)	-0.0092(0.0012)	0.0043(0.0003)	0.0057(0.0004)	0.0007(0.0000)	0.0044(0.0003)	-0.0266(0.0097)	-0.0267(0.0098)
ν_{109}(0.2028)	0.1362(0.2254)	0.1400(0.2381)	0.2116(0.5446)	0.1260(0.1930)	0.1287(0.2013)	0.0185(0.0042)	0.1292(0.2031)	0.1294(0.2037)
ν_{113}(0.2043)	-0.0373(0.0167)	-0.0479(0.0275)	0.0178(0.0038)	0.0004(0.0000)	-0.0270(0.0088)	0.0087(0.0009)	0.0396(0.0188)	0.0719(0.0620)
ν_{118}(0.2206)	0.1599(0.2626)	0.1453(0.2170)	0.0374(0.0144)	0.1832(0.3447)	0.1850(0.3518)	0.0734(0.0554)	0.0945(0.0917)	0.0939(0.0905)
ν_{120}(0.3928)	0.0016(0.0000)	0.0025(0.0000)	0.0001(0.0000)	0.0004(0.0000)	0.0012(0.0000)	0.0004(0.0000)	0.0030(0.0000)	0.0029(0.0000)
ν_{124}(0.3951)	0.0029(0.0000)	0.0040(0.0001)	0.0000(0.0000)	0.0011(0.0000)	0.0023(0.0000)	0.0007(0.0000)	0.0040(0.0001)	0.0039(0.0000)
ν_{128}(0.3967)	-0.0133(0.0006)	-0.0192(0.0012)	0.0000(0.0000)	-0.0051(0.0001)	-0.0101(0.0003)	-0.0001(0.0000)	-0.0249(0.0020)	-0.0249(0.0020)
ν_{132}(0.3988)	-0.0029(0.0000)	-0.0040(0.0000)	-0.0103(0.0003)	-0.0012(0.0000)	-0.0040(0.0001)	-0.0095(0.0003)	-0.0043(0.0001)	-0.0043(0.0001)

Table 4. Total stabilization energy (in eV) for low lying excited states of R-NDI

State	H-NDI	Me-NDI	Ph-NDI
S_1	0.22	0.23	0.31
S_2	0.23	0.19	0.33
T_1	0.30	0.30	0.30
T_2	0.21	0.11	0.26
T_3	0.11	0.22	0.27
T_4	0.22	0.23	0.14
T_5	0.22	0.24	0.30
T_6	0.17	0.19	0.29

E_{st} of S_1 is estimated to be ~0.22, ~0.23 and ~0.31 eV for H-NDI, Me-NDI and Ph-NDI, respectively. We found that the major contribution (~20%) to this energy is originating from C=O symmetric stretch (n_{66}) vibrational mode.

Also, similar E_{st} values found for S_2 of NDIs. These E_{st} values suggest that the geometrical distortions in S_1 and S_2 are not severe, as is expected due to their rigid polycyclic skeletal structure.

Finally, the global minimum of a given electronic state is estimated by subtracting the E_{st} from FC vertical energy. Estimated global minima of electronic states of NDIs are plotted in Fig. 5.

Energy gap trends of electronic state minima (*cf.* Fig. 5), suggest that T_4 and T_5 to be the receiver triplet states, same as at FC geometry, for ISC occurring via S_1 and S_2 states, respectively, in H-NDI. On the other hand, T_5 in Me-NDI and T_3 in Ph-NDI to be the receiver triplet state for ISC via S_1. Similarly, T_6 in Me-NDI and T_3 in Ph-NDI are found more relevant for ISC via S_2.

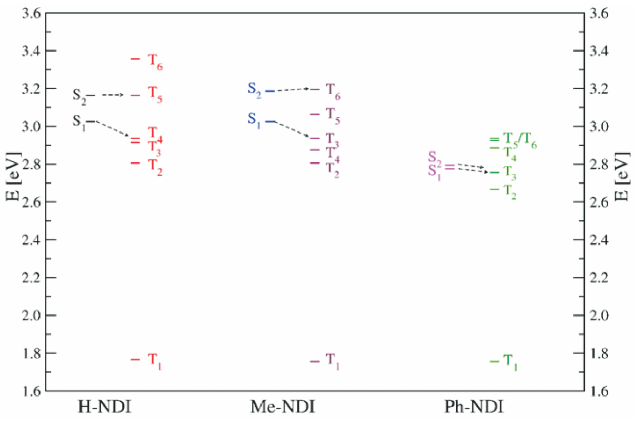

Fig. 5. Equilibrium minimum energies of low-lying electronic states of R-NDI computed at TD-B3LYP/6-311G* level of theory. Energetically favorable ISC pathways are shown with arrow symbol.

In summary, high-lying triplet states (T_3-T_6) are responsible for ISC originating either at respective FC point or at equilibrium minimum of S_1 and S_2 of R-NDIs. All these involved states lie ~4000 cm^{-1} above T_2, indicating a minimal or no direct participation of T_2 (and T_1) in ISC of NDIs.

Assuming the energetics and associated ISC pathways of rNDI to be same as that of R-NDI, then an enhancement of ISC efficiency is thus expected for rNDI due to heavy-atom effect[13]. Furthermore, presence of Br atom and core-substitution may induce additional electronic effects thereby resulting in various unexpected ISC pathways in rNDI. Future studies are aimed in this direction to provide an accurate understanding of photophysical properties of rNDI.

Conclusions

Energetics of involved singlet-triplet manifold play a key role in molecules exhibiting ultrafast intersystem crossing process in the absence of a heavy atom. Our findings on low-lying singlet-triplet manifold clearly indicate the minimal or no direct participation of T_1 and T_2 states in ISC in NDIs. Higher receiver triplet states (T_n, n > 2), isoenergetic with S_1 and S_2, have to be considered for interpreting the mechanistic details of ISC in NDIs.

The insights obtained from our study may pave the way for a better understanding of photophysical processes of NDIs[14–16] and trigger new experimental and theoretical studies to control and design optoelectronic materials[17,18].

Acknowledgements

This project is funded by Science and Engineering Research Board (SERB), Department of Science and Technology (DST), Government of India (File No. ECR/2016/000226). SVK acknowledges DST for INSPIRE-PhD fellowship.

References

1. N. J. Turro, "Modern Molecular Photochemistry", University Science Books, Mill Valley, CA, 1991.
2. O. Yushchenko, G. Licari, S. Mosquera-Vazquez, N. Sakai, S. Matile and E. Vauthey, *J. Phys. Chem. Lett.*, 2015, **6**, 2096.
3. R. Englman and J. Jortner, *Mol. Phys.*, 1970, **18**, 145.
4. K. F. Freed and J. Jortner, *J. Chem. Phys.*, 1970, **52**, 6272.
5. L. S. Cederbaum, *J. Chem. Phys.*, 1983, **78**, 5714.
6. L. S. Cederbaum, H. Köppel and W. Domcke, *Int. J. Quant. Chem.*, 1981, **S15**, 251.
7. V. S. Reddy and S. Irle, *J. Chem. Theory Comput.*, 2017, **13(10)**, 4944.
8. (a) A. D. Becke, *J. Chem. Phys.*, 1992, **96**, 2155; (b) A. D. Becke, *J. Chem. Phys.*, 1992, **97**, 9173; (c) C. Lee, W. Yang and R. G. Parr, *Phys. Rev. B*, 1988, **37**, 785.
9. M. J. Frisch, G. W. Trucks, H. B. Schlegel, G. E. Scuseria, M. A. Robb, J. R. Cheeseman, G. Scalmani, V. Barone, G. A. Petersson, H. Nakatsuji, X. Li, M. Caricato, A. Marenich, J. Bloino, B. G. Janesko, R. Gomperts, B. Mennucci, H. P. Hratchian, J. V. Ortiz, A. F. Izmaylov, J. L. Sonnenberg, D. Williams-Young, F. Ding, F. Lipparini, F. Egidi, J. Goings, B. Peng, A. Petrone, T. Henderson, D. Ranasinghe, V. G. Zakrzewski, J. Gao, N. Rega, G. Zheng, W. Liang, M. Hada, M. Ehara, K. Toyota, R. Fukuda, J. Hasegawa, M. Ishida, T. Nakajima, Y. Honda, O. Kitao, H. Nakai, T. Vreven, K. Throssell, J. A. Montgomery (Jr.), J. E. Peralta, F. Ogliaro, M. Bearpark, J. J. Heyd, E. Brothers, K. N. Kudin, V. N. Staroverov, T. Keith, R. Kobayashi, J. Normand, K. Raghavachari, A. Rendell, J. C. Burant, S. S. Iyengar, J. Tomasi, M. Cossi, J. M. Millam, M. Klene, C. Adamo, R. Cammi, J. W. Ochterski, R. L. Martin, K. Morokuma, O. Farkas, J. B. Foresman and D. J. Fox, Gaussian 09, Revision A.02, Gaussian, Inc., Wallingford CT, 2009.
10. W. Domcke, D. R. Yarkony and H. Koppel, "Conical Intersections: Electronic Structure, Dynamics and Spectroscopy", World Sci., Singapore, 2004, **7**, pp. 323-368.
11. E. B. Wilson, J. C. Decius and P. C. Cross, "Molecular vibrations", McGraw-Hill, New York, 1955.
12. H. Köppel, W. Domcke and L. S. Cederbaum, *Adv. Chem. Phys.*, 1984, **57**, 59.
13. N. J. Turro, V. Ramamurthy and J. C. Scaiano, "Principles of Molecular Photochemistry, An Introduction", University Science Books, First Indian Edition, 2015.
14. P. Ganesan, J. Baggerman, H. Zhang, E. J. R. Sudholter and H. Zuilhof, *J. Phys. Chem. A*, 2007, **111(28)**, 6151.
15. N. Sakai, J. Mareda, E. Vauthey and S. Matile, *Chem. Commun.*, 2010, **46**, 4225.
16. S. Alp, S. Erten, C. Karapire, B. Koz, A. O. Doroshenko and S. Icli, *J. Photochem. Photobiol. A*, 2000, **135**, 102.
17. F. Wurther, S. Ahmed, C. Thalacker and T. Debaerdemaeker, *Chem. Eur. J.*, 2002, **8**, 4742.
18. A. L. Sisson, N. Sakai, N. Banerji, A. Furstenberg, E. Vauthey and S. Matile, *Angew. Chem., Int. Ed.*, 2008, **47**, 3727.